Journal of Hepatocellular Carcinoma

Dovepress

open access to scientific and medical research

Open Access Full Text Article

ORIGINAL RESEARCH

Inhibitory Effects of Esculetin on Liver Cancer Through Triggering NCOA4 Pathway-Mediation Ferritinophagy in vivo and in vitro

Zhiru Xiu[1], Yiquan Li[1], Jinbo Fang[1], Jicheng Han[1], Shanzhi Li[1], Yaru Li[1,2], Xia Yang[1], Gaojie Song[3], Yue Li[1], Ningyi Jin[1,4,5], Yilong Zhu[1], Guangze Zhu[1], Lili Sun[6], Xiao Li[1,4,7]

[1]Academician Workstation of Jilin Province, Changchun University of Chinese Medicine, Changchun, People's Republic of China; [2]Medical College, Yanbian University, Yanji, People's Republic of China; [3]Medical College, Jiujiang · University, Jiujiang, People's Republic of China; [4]Changchun Veterinary Research Institute, Chinese Academy of Agricultural Sciences, Changchun, People's Republic of China; [5]Jiangsu Co-Innovation Center for Prevention and Control of Important Animal Infectious Diseases and Zoonoses, Yangzhou, People's Republic of China; [6]Department of Head and Neck Surgery, Tumor Hospital of Jilin Province, Changchun, People's Republic of China; [7]College of Life Sciences, Shandong Normal University, Jinan, People's Republic of China

Correspondence: Lili Sun; Xiao Li, Boshuo Road, 1035, Jingyue Economic & Technological Development Zone, Changchun, Jilin, 130122, People's Republic of China, Tel +86-431-86985923, Fax +86-431-87985861, Email skylee6226@163.com; linjiaxiaoya@163.com

Objective: To explore the effects of Esculetin on liver cancer and explore potential mechanisms of Esculetin-inducing cells death.

Methods: Esculetin's effects on the proliferation, migration and apoptosis of HUH7 and HCCLM3 cells were detected by using CCK8, crystal violet staining, wound healing, Transwell^{TM} and Annexin V-FITC/PI. Flow cytometry, fluorescence staining, Western blot, T-AOC, DPPH radical scavenging assay, hydroxyl radical's inhibitory capability and GSH test were used to examine the esculetin's effects on the ROS level, the oxidation-related substances and proteins' expression in hepatoma cells. In vivo experiment was performed by xenograft model. Ferrostatin-1 was used to determine the death way of hepatoma cells induced by esculetin. Live cell probe, Western blot, Fe^{2+} content, MDA, HE staining, Prussian blue staining and immunohistochemistry were used to examine the ferritinophagy-related phenomenon induced by esculetin in hepatoma cells. The relationship between esculetin and NCOA4-mediated ferritinophagy was confirmed through gene silence and overexpression, immunofluorescence staining and Western blot.

Results: Esculetin suppressed the proliferation, migration and apoptosis of HUH7 and HCCLM3 cells significantly, influenced the oxidative stress level, altered the autophagy and iron metabolism levels in cells, and produced a ferritinophagy-related phenomena. Esculetin increased the levels of cellular lipid peroxidation and reactive oxygen species. In vivo, esculetin could decrease tumour volume, promote LC3 and NCOA4 expressions, suppresse hydroxyl radical's inhibiting capacity and GSH, increase Fe^{2+} and MDA levels, decrease antioxidant proteins expression in tumour tissue. In addition, Esculetin could also increase the iron deposition of tumour tissues, promote ferritinophagy, and induce tumours' ferroptosis.

Conclusion: Esculetin has an inhibitory effect on liver cancer in vivo and in vitro through triggering NCOA4 pathway-mediation ferritinophagy.

Keywords: esculetin, ferritinophagy, liver cancer, anti-tumour, NCOA4

Introduction

Ferroptosis is a non-apoptotic, iron-dependent form of cell death characterized by the accumulation of lipid peroxides.[1] Its foundation is active iron, which can be produced through the ferritinophagy pathway.[2] Ferritinophagy is a new type of autophagy that relies on the nuclear receptor coactivator 4 (NCOA4), a receptor that can transport ferritin to autophagosomes and interact with them. Ferritin is degraded into active iron through lysosome fusion.[3–5] When cells experience iron overload, the Fenton reaction increases the level of reactive oxygen species (ROS) and interacts with polyunsaturated fatty acids (PUFA) on the cell membrane to promote lipid peroxidation. This process results in the accumulation of cellular lipid peroxides, leading to cellular ferroptosis.[6–8] Glutathione peroxidase 4 (GPX4) is a key antioxidant enzyme

Received: 8 November 2022
Accepted: 18 January 2023
Published: 11 April 2023

that turns reduced GSH to oxidized GSH, while also transforming harmful lipid peroxides into harmless lipid alcohols. GSH depletion and GPX4 inactivation are key events in triggering lipid peroxidation during ferroptosis.[9–11]

According to reports, the incidence and mortality of liver cancer are seriously endangering in human health and life.[12] Currently, the treatment of liver cancer is primarily multidisciplinary and relies on multi-treatment approaches, such as surgery, ablation, hepatic arterial chemoembolization and systemic therapy.[13–15] Although advances have been made, nearly 70% of patients do not benefit. Due to the advanced stage of diagnosis, these patients are prone to recurrence after surgery and only liver transplantation can be used for a very limited group of patients.[16,17] For patients who cannot have hepatectomy, the development of targeted drugs, such as sorafenib and Lenvatinib, brings hope to advanced liver cancer patients, but these drugs can only prolong patients' lives by 2–3 months.[18,19] As a response, there is a pressing need to discover and develop a new approach for the clinical drug treatment of patients with advanced liver cancer. Esculetin, also known as 6,7-dihydroxycoumarin, is a coumarin derivative, extracted from *Lemon* leaves, Rehmannia glutinosa (*Rehmannia glutinosa var.*), belladonna (*Belladonna baccifera Lam*.) and other plants.[20,21] Esculetin has been shown to have a variety of therapeutic activities, such as for the treatment of diabetes, intestinal diseases and liver protection. It also has antibacterial and anti-inflammatory effects.[22–25] In recent years, esculetin has garnered extensive attention for its use in tumour therapy, as it has been shown to have therapeutic effects on leukaemia, glioma, prostate, colon, pancreatic, melanoma, breast and gastric cancers,[24–32] Some researchers found that esculetin induces ROS formation and activates apoptosis in gastric cancer cells.[33] Esculetin acts on PGK2, GPD2 and GPI to prevent cancer cells from undergoing glycolysis.[34] However, there are few studies on the effect of esculetin in inducing ferritinophagy in hepatoma cells. As a result, this study aimed at evaluating the efficacy of esculetin in inducing cell ferroptosis via ferritinophagy in liver cancer and at exploring its potential mechanisms.

Materials and Methods

Antibodies and Reagents

NFE2L2 (16396-1-AP) and LC3II (14600-1-AP) were purchased from proteintech. HO-1 (86806, CST), FTH1 (4393, CST), Gpx4 (PA5-102521, Invitrogen), NCOA4 (HC071-1F11, Sigma-Aldrich).

Esculetin, Cisplatin and Sorafenib (MCE, USA), T-AOC Assay, ROS Assay Kit, Crystal Violet Staining Solution, Lyso-Tracker Red (Solarbio, China), Mito-Tracker (Beyotime, China), DPPH free radical scavenging rate detection kit (Leagene, China), Transwell^{TM} polycarbonate membrane cell culture inserts (Corning, Germany), Liperfluo, FerroOrange, Cell Counting Kit-8 (DOJINDO, Japan), GSH (reduced glutathione) determination kit (NJJCBIO).

Transfection and Cell Culture

The human hepatoma (Chinese Academy of Sciences, China) HUH7 and HCCLM3 cells were cultured in an incubator at 5% CO_2, 37°C. DMEM (1% 50 U/mL penicillin) with 10% FBS was used to culture cells. In following experiments, the cells were used to do following detection, when the cell concentration was increased to 80%.

For the experiment's purposes, the si-LC3II or si-NCOA4 were chose with silent effects. The siLC3II and siNCOA4 (RIBOBIO, China) sequences are 5′-GAAGGCGCUUACAGCUCAATT-3′ and 5′-CAACTGTCCTGCTCTTTGA-3′. 50 nM siRNA was used to transfect to HUH7 and HCCLM3 cells reference to the instruction. pCDNA 3.1 plasmid of FTH1 (fenghuishengwu, China) was selected for an overexpression effect. Using DNA transfection reagent (Roche's X-tremeGENE), plasmid of FTH1 and control were used to transfect to HUH7 and HCCLM3 cells.

Experimental Animals

We bought female BALB/c nude mice when they were 4–5 weeks old from Beijing Shenghe Experimental Animal Technology Co., Ltd., at the end of treatment, from each group, 3 nude mice were killed by cervical dislocation at random, the others were euthanized. The AVMA's rules for animal euthanasia were followed while performing the euthanasia process. Euthanasia was accomplished with a continuous 2–3min intraperitoneal delivery of 3 times pentobarbital sodium dosage (150mg/kg).

Proliferation Assay

The HUH7 and HCCLM3 cells were planted in a 96-well plate about per well 1×10^4 cells. Esculetin is made into various concentrations and then added to each well, treatment time was 12, 24, 48 or 72 h, whereas the control group was cultured normally using the same solvents (DMEM medium containing 1/1000 volume of DMSO) and time. At end of treatment, 10 μL reagent of CCK-8 was added. After 2h, the OD value at 450 nm was determined by microplate reader, the effective concentration of a low dose (20 μM, ESCL group), medium dose (40 μM, ESCM group) and high dose (60 μM, ESCH group) and time (48h) were selected for subsequent experiments.

Crystal Violet

The cells were therapied with varying doses of esculetin for 48 h in 12-well plates. 0.1% crystal violet was used to stain cells for 10 min. The cells were photographed after being washed with PBS.

Cell Migration

The cells were therapied with varying doses of esculetin for 48 h in 12-well plates. The cells were wounded with a tip in the middle of the well, washed with PBS, then added to DMEM, the scratch healing degree was examined, respectively, at 0, 24 and 48 h.

The cells were re-suspended in DMEM with 0.5% FBS. 24-well plates were used to hold the Transwell™ chamber. 2000 cells about 200 μL were put in the top of Transwell™ chamber. 500 μL 10% FBS DMEM was put in the lower part of the Transwell™ chamber and cultured for 24 h at 37 °C, 5% CO_2. Following the completion of the culture, 0.1% crystal violet was used to stain the chambers for 5 min. The Transwell™ chamber was taken pictures under a 20× microscope, after being cleaned with PBS. The number dissimilarity of cells passed through the membrane reflects in the migration capacity of tumor.

Apoptosis Assay

The cells were therapied with varying doses of esculetin for 48 h in 12-well plates. The DMEM and cells were collected, centrifuged and re-suspended in 1 mL binding buffer, stained for 20 min with 10 μL Annexin V-FITC/PI at room temperature, then flow cytometry was performed to measure.

T-AOC Assay

The cells were therapied with varying doses of esculetin for 48 h in 12-well plates. 10^6 cells were collected, put in 200 μL cold PBS, centrifuged at 4°C, 12,000 g for 5 min, the supernatant was taken for further examination, results were computed.

DPPH Free Radical Scavenging

The cells were therapied with varying doses of esculetin for 48 h in 12-well plates. The cells were collected for ultrasonic fragmentation and 10 min centrifugation, 0.8mL of nitrogen-free radical extract was given to every 5×10^6 cell, the supernatant was taken for further examination, and results were computed.

ROS Assay

The cells were therapied with varying doses of esculetin for 48 h in 12-well plates. The 10 μM DCFH-DA probe was added to cells and cultured at 37°C for 20 min. Ensure the probe fully contact with the cell by turning the mixture upside down every 3–5 min. The cells were detected by flow cytometry and a confocal microscope.

Lipid Peroxidation

The cells were therapied with varying doses of esculetin for 48 h in 12-well plates. The lipid peroxidation probe was mixed with 2 mL serum-free DMEM. After 30 min at 37 °C, the cells and DMEM were collected, then identified by confocal microscope and flow cytometry.

FerroOrange

The cells were therapied with varying doses of esculetin for 48 h in 12-well plates. The cells were washed with DMEM. FerroOrange probe was mixed with serum-free DMEM and cultivated cells for 30 min. After that, removed the DMEM, washed the cells 3 times with HBSS and acquired confocal microscopy pictures.

Mitochondria and Lysosomes Co-Stain

The cells were therapied with varying doses of esculetin for 48 h in 12-well plates. The 100 nM LTR (Lyso-Tracker Red) and MTG (Mito-Tracker Green) probes were added to cells. Following a 30 min culture at 37°C, the cells were washed 3 times with PBS and acquired pictures using confocal microscopy.

JC-1 Staining

The cells were therapied with varying doses of esculetin for 48 h in 12-well plates. The JC-1 probes were mixed to the DMEM. Following a 30 min culture at 37°C, the cells were washed 3 times with PBS and acquired confocal microscopy pictures.

Western Blot

The cells were therapied with varying doses of esculetin for 48 h in 12-well plates. Total proteins were collected by kit (Kang Wei Century, Beijing) and measured by BCA kit (Beyotime, Shanghai), then marked sample to electrophoresis and membrane transfer. 5% low-fat milk shaking 2 h. The membrane was incubated in the primary antibody overnight at 4°C, then incubated in second antibody about 1 h at room temperature. Finally, the imaging system and ECL kit (Thermo, USA) were used to determine the level of protein, GAPDH is the reference.

Immunofluorescence

The cells were therapied with varying doses of esculetin for 48 h in 12-well plates. After fixed 30 min in 4% paraformaldehyde, the cells were mixed with 1% BSA (0.5% Triton) for 2 h at room temperature. First antibody was added in cells overnight at 4 °C, then put cells in the secondary antibody tagged by FITC or CY3 for 1 h before the cells were identified by fluorescence microscope.

Xenotransplantation

1×10^7/mL HUH7 cells were suspended and implanted into the 5-week-old BALB/c (n=6) nude mice right hindlimb, the entire procedure was kept aseptic. Growth of tumours was observed daily following tumour formation. When irregular patches were felt after 7 days, the model was effectively established. Then, mice were divided into 6 groups at random: control (equal volume solvent), sorafenib (30 mg/kg), cisplatin (5 mg/kg) or esculetin (10, 30, 60 mg/kg). The body weight and tumour volume of nude mice were monitored every 3 days. The mice were done to death after treatment for 14 days, the tumours and 5 internal organs were stored in 4% paraformaldehyde and detected using H&E, immunohistochemical and Prussian blue stain.

$$\text{Tumour volume}\left(\text{mm}^3\right) = \left(\text{long diameter of tumour} \times \text{short diameter of tumour}^2\right)/2$$

The inhibition rate formula:

$$\text{Tumour inhibition rate} = (1 - \text{treatment group tumour volume}/\text{control tumour volume}) \times 100\%$$

Prussian Blue Stain

The tumor tissues were stored in 4% paraformaldehyde, carried out the relevant pathological procedure processing, cut into 5μm thick pieces. Prussian blue stain was done in 37°C distilled waters for 5 min according to instructions. Then, the Prussian blue stain fragments were viewed, photographed and analyzed under a microscope.

H&E Stain

The tumor tissues were stored in 4% paraformaldehyde, carried out the relevant pathological procedure processing, cut into 5μm thick pieces, according to H&E staining instructions, pieces were viewed, photographed and analyzed under a microscope.

Immunohistochemistry

The tumor tissues were stored in 4% paraformaldehyde, carried out the relevant pathological procedure processing, cut into 5μm thick pieces, dehydrated, removed endogenous peroxidase activity, put in BSA for 30 min. Following incubation with the antibodies, according to immunohistochemistry instructions, pieces were sealed and viewed, photographed and analyzed under a microscope. Utilizing the same yellow-brown as the standard for measuring positive immunostaining, the image-ProPlus6.0 system assessed immunostaining to determine each picture IOD (cumulative light intensity, density), AREA (pixel tissue area) and mean density (IOD/AREA average density).

Biochemical Assay

Reference to the biochemical kit instructions, MDA (malondialdehyde), GSH (reduced glutathione), OH· (hydroxyl radical) (Nanjing Jiancheng, China) and the level of Fe^{2+} (Leagene, China) in serum were measured.

Statistical Analysis

The data is supplied in the form of mean SD (standard deviation) values. The results from at least three different experiments were statistically analysed. Analysis of variance (ANOVA) of unpaired double-tailed student's-test was performed by using the GraphPadPrism 6.0. *$p<0.05$ is statistically significant.

Results

Esculetin's Effect on Hepatocellular Cancer Cells

Esculetin was shown to inhibit hepatoma cell growth. The CCK8 assay (Figure 1A and B) revealed that esculetin suppresses the proliferation of HUH7 and HCCLM3 cells in a dose- and time-dependent manner. When the concentration of esculetin was used at 40μM for 48 h, the inhibition rate was 34.30 ± 8.95% for HUH7 cells and 70.45 ± 14.80% for HCCLM3. As a result, for later tests, we selected 20 μM as a low dose (ESCL group), 40 μM as a medium dose (ESCM group) and 60 μM as a high dose (ESCH group) and the treatment time was selected as 48h. A dose-dependent reduction in adherent cells in the treatment group was noticed by crystal violet staining (Figure 1C). Transwell™ and scratch migration assays were used to assess esculetin's effects on the migration of HUH7 and HCCLM3 cells. According to the results, esculetin suppressed HUH7 and HCCLM3 cells migration (Figure 1D–G) in a dose-related manner. The outcomes show that esculetin could prevent HUH7 and HCCLM3 cells' proliferation and migration.

Esculetin's Effects on Apoptosis and ROS Production in Hepatocellular Cancer Cells

To investigate the mechanisms by which esculetin limits HUH7 and HCCLM3 cells' growth, flow cytometry was used to identify the apoptosis of the cells after the addition of esculetin. We found that HUH7 and HCCLM3 cells after esculetin treated and showed significant apoptosis and necrosis (Figure 2A–C). The apoptotic rates of HCCLM3 cells in the treatment groups (ESCL, ESCM and ESCH) were 5.4%, 7.6% and 7.3%, the rates of necrosis were 18.8%, 24.3% and 32.8%, respectively. The apoptotic rates of HUH7 cells in the treatment groups were 8%, 9.3% and 15.8%, the rates of necrosis were 3.2%, 4.3% and 2.6%, respectively. Additionally, we found that after 48 h of treatment with esculetin, HUH7 and HCCLM3 cells generated considerably more ROS when seen under a fluorescence microscope (Figure 2D and E). A similar finding was made using flow cytometry (Figure 2F).

Esculetin's Effects on Oxidative Stress State in Hepatocellular Cancer Cells

ROS[35–37] was shown to be directly connected to the amount of oxidative stress. Therefore, we measured oxidation level within the cells. Esculetin dramatically decreased DPPH free radicals scavenging rate and suppressed total antioxidant capacity (T-AOC)

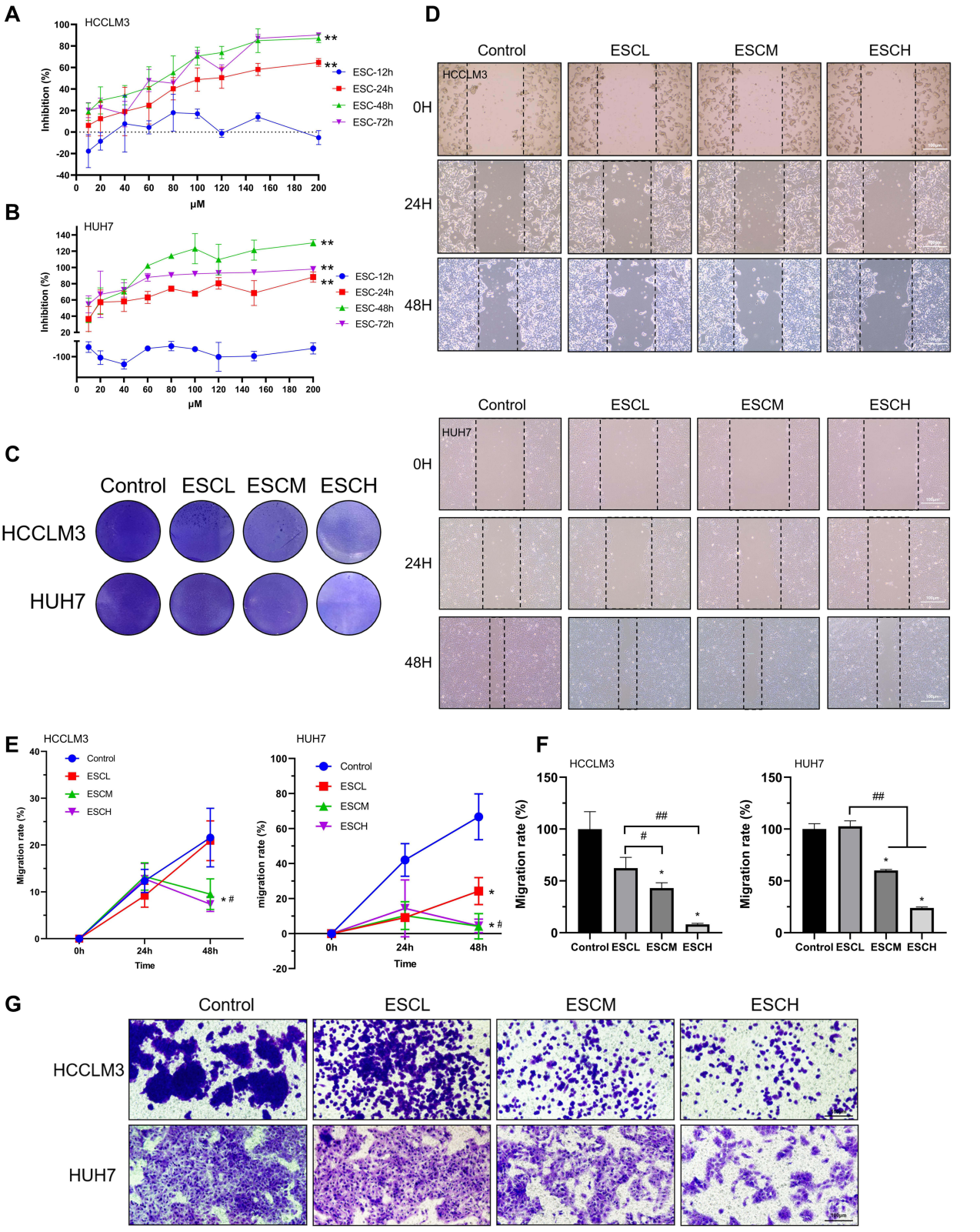

Figure 1 Esculetin's effect on HUH7 and HCCLM3 cells. (**A** and **B**) Esculetin's inhibition time (12, 24, 48 or 72h) and concentration (10–200 μM) on HUH7 and HCCLM3 cells was screened using the CCK8 assay. (**C**) Esculetin's ability to suppress cells was displayed by crystal violet. (**D** and **E**) Using the wound healing assays and (**F** and **G**) the Transwell ™, the effects of esculetin on cells migration were examined. The results were displayed as mean ± SD. Compared with the Control group, *p<0.05, **p<0.01. Compared with the ESCL group, #p<0.05, ##p<0.01. Compared with the ESC-12h group, *p<0.05, **p<0.01 in A and B.

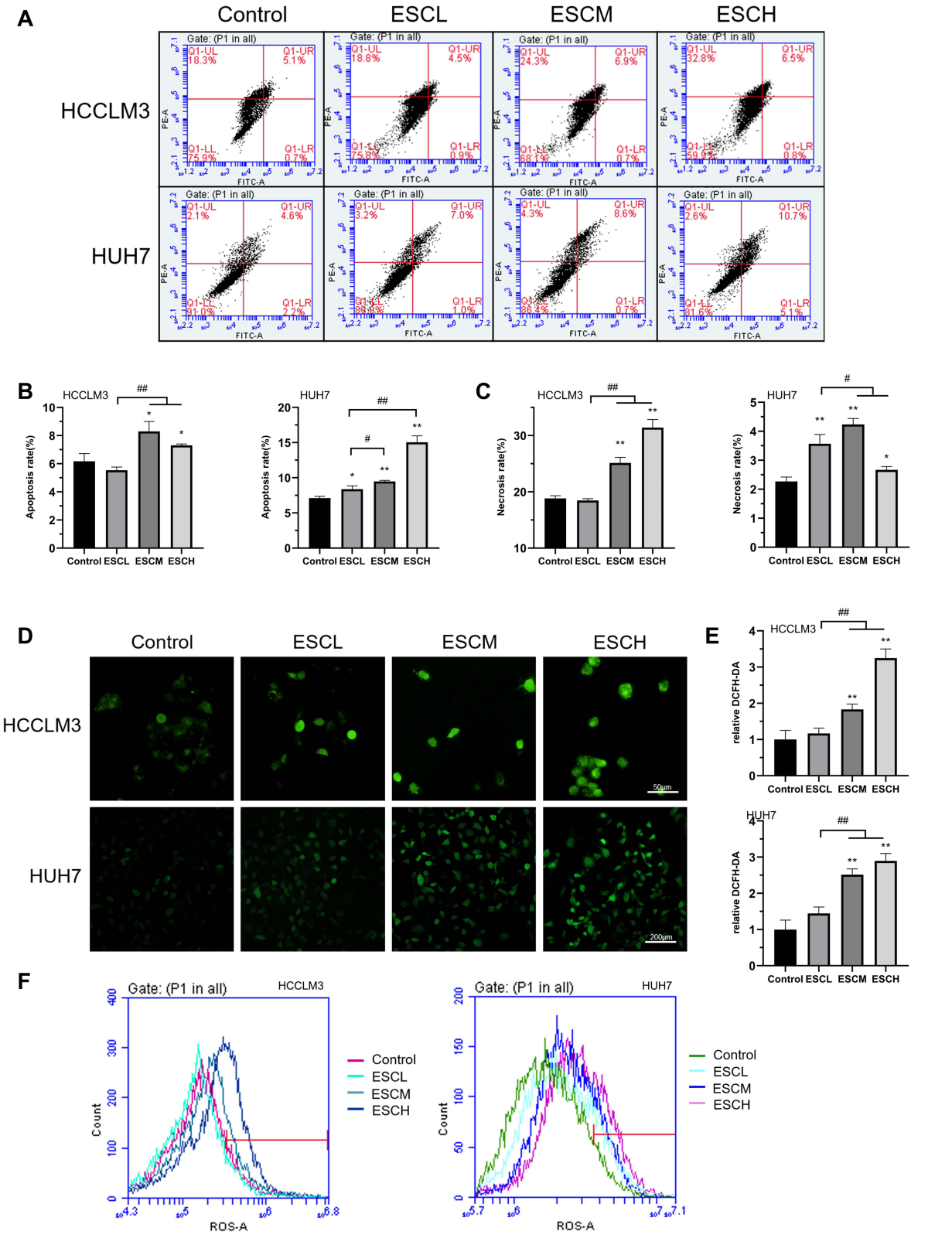

Figure 2 Esculetin induces apoptosis and ROS production in HUH7 and HCCLM3 cells. (**A**) Annexin V-FITC/PI in cells was detected by flow cytometry and the outcomes are represented by the (**B**) apoptosis rate and (**C**) necrosis rate. ROS in cells was observed using confocal microscopy (**D** and **E**) and flow cytometry (**F**). The results are displayed as mean ± SD. Compared with the Control group, *p<0.05, **p<0.01. Compared with the ESCL group, #p<0.05, ##p<0.01.

(Figure 3A and B) in hepatocellular cancer cells. The levels of antioxidant proteins (NFE2L2, GPX4 and HO-1) were considerably lower than the control group in the ESCM and ESCH groups, according to Western blot analysis (Figure 3C and D). Consequently, esculetin effectively suppresses antioxidant level and proteins expressions in HUH7 and HCCLM3 cells.

Esculetin's Effects on Lysosomes, Fe^{2+} and Ferrostatin-1 in Hepatocellular Cancer Cells

ROS are closely linked to autophagy and ferroptosis.[38,39] After incubation with esculetin for 48 hours, we found that ferrostatin-1, a ferroptosis inhibitor, bafilomycin and 3-MA could inhibit esculetin-mediated cell death (Figure 4A),

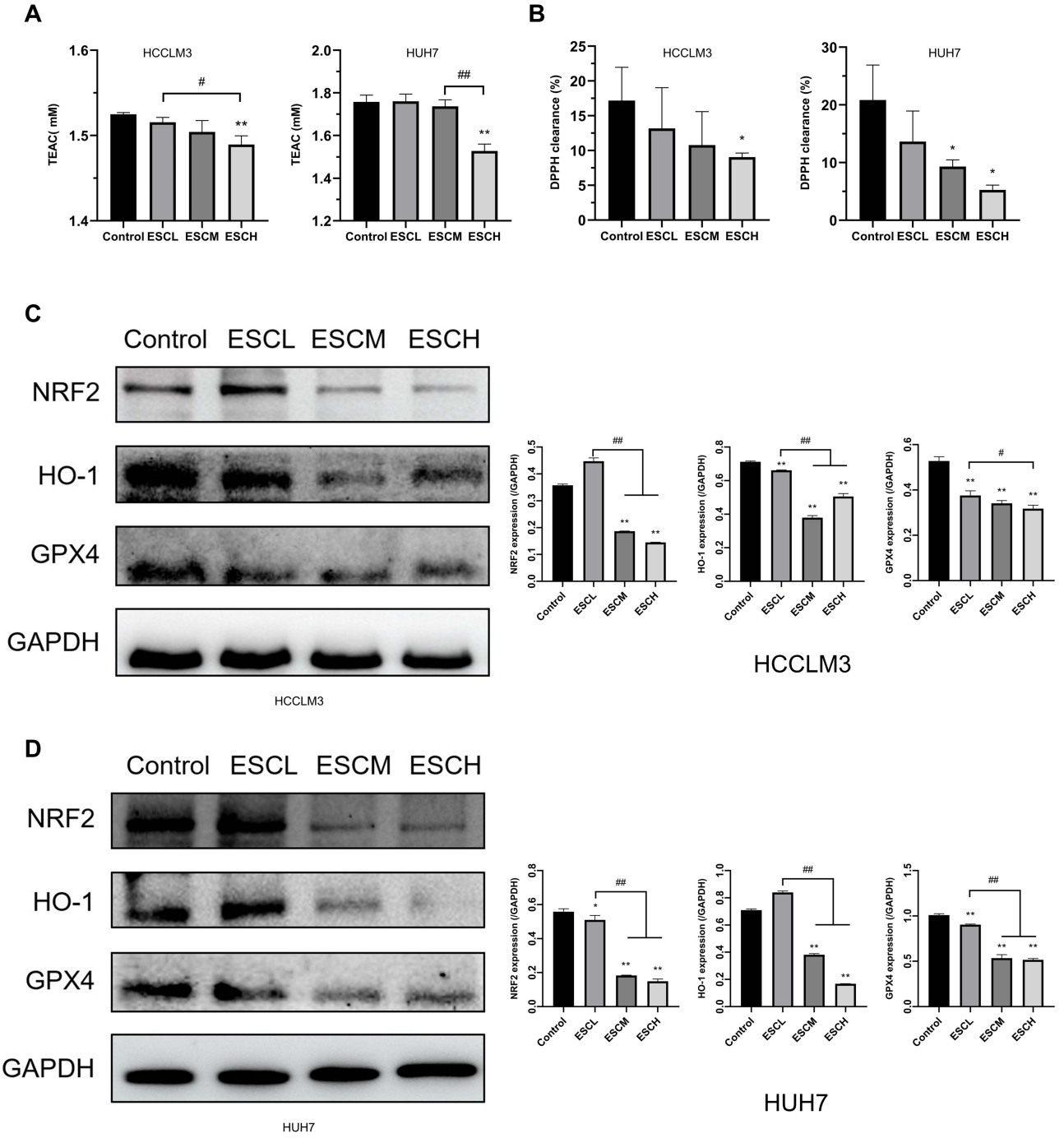

Figure 3 Esculetin's effects on antioxidant levels in HUH7 and HCCLM3 cells. The ability of cells to produce antioxidants was evaluated using the (**A**) T-AOC assay and (**B**) DPPH free radical scavenging rate. (**C** and **D**) The proteins expressions of cells antioxidation were examined by Western blot. The results are displayed as mean ± SD. Compared with the Control group, *p<0.05, **p<0.01. Compared with the ESCL group, #p<0.05, ##p<0.01.

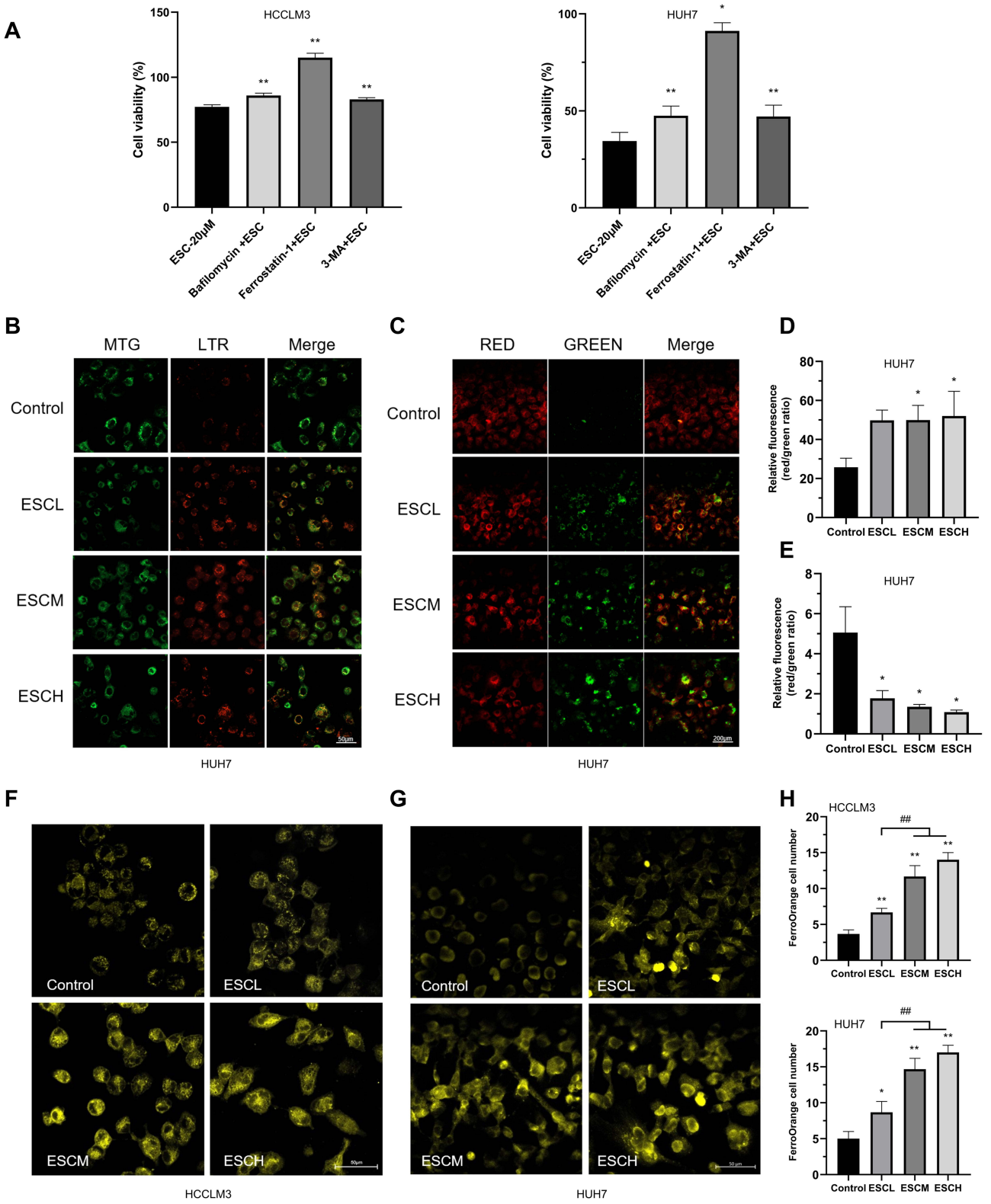

Figure 4 Esculetin's effects on lysosomes, Fe^{2+} and ferroptosis in HUH7 and HCCLM3 cells. (**A**) The CCK8 assay was used to examine whether ferrostatin-1, bafilomycin and 3-MA could influence efficacy of esculetin on HUH7 and HCCLM3 cells. (**B** and **D**) Utilizing co-staining of MTG and LTR analyzed the autophagy-lysosome state in cells. (**C** and **E**) Utilizing JC-1 stain examined the state of the cells' mitochondrial membrane potential. (**F–H**) Utilizing the FerroOrange probe, Fe^{2+} level in cells were measured. The results are displayed as mean ± SD. Compared with the Control group, *p<0.05, **p<0.01. Compared with the ESCL group, ##p<0.01. Compared with the ESC- 20μM in A, *p<0.05, **p<0.01.

suggesting that esculetin induces ferroptosis and autophagy. It was previously shown that an excess of Fe^{2+} can cause a rise in ROS.[40–42] After incubation with esculetin for 48 hours, we used the FerroOrange live cell probe to measure the iron content of HUH7 and HCCLM3 cells and found that the level of Fe^{2+} is substantially increased (Figure 4F–4H). We also observed significant alterations in mitochondrial membrane potential using the JC-1 staining (Figure 4C and E). MTG (Mito-Tracker) and LTR (Lyso-Tracker Red) co-staining were used to determine the effects of esculetin on lysosomes and mitochondria in cells. The mitochondria green fluorescence reduced and the lysosomes' red fluorescence (Figure 4B and D) were enhanced in a dose-related manner. Those findings implied that esculetin causes mitochondria damage, which is also responsible for the rise of ROS levels. Meanwhile, the rise in lysosomes and the decrease of cell inhibition rate following inhibitor treated demonstrated that esculetin could cause an increase in autophagy. These findings suggest that esculetin may induce ferroptosis and autophagy in HUH7 and HCCLM3 cells.

Esculetin's Effects on Lipid Peroxidation and Ferritinophagy-Proteins in Hepatocellular Cancer Cells

Several investigations have revealed that intracellular iron excess may result in the production of intracellular lipid peroxidation,[43,44] which influences the level of intracellular autophagy.[11,45,46] Using Liperfluo probe, the results confirmed that after 48 hours of incubation with esculetin, the amount of intracellular lipid peroxidation considerably increased (Figure 5A). Flow cytometry results confirmed the confocal microscopy results (Figure 5B). Esculetin dramatically upregulated the levels of NCOA4 and LC3-II in HUH7 and HCCLM3 cells, but suppressed FTH1 expression (Figure 5C and D). Esculetin dramatically suppressed p62 expression, but after bafilomycin (Baf) and ESCM co-treatment, dramatically upregulated p62 expression (Figure 5E), suppressed LC3-II expression, suggested Esculetin can promote autophagy flux. In conclusion, esculetin causes cell death, suppresses cell growth and activates ferritinophagy in HUH7 and HCCLM3 cells.

NCOA4, LC3II and FTH1 Proteins are Essential for Esculetin-Induced Ferritinophagy in Hepatocellular Cancer Cells

To evaluate whether esculetin promotes ferritinophagy, we applied immunofluorescence to detect NCOA4 and LC3-II co-localization (Figure 6C and D). Following treatment with esculetin (ESC,60 μM) for 48 hours, there were several bright green spots that were observed in HUH7 and HCCLM3 cells of the ESC group, suggesting an increase in LC3-II expression. Higher red fluorescent spots suggested an increase in NCOA4 expression, whereas the increase in yellow spots indicated a colocalization between LC3-II and NCOA4 and suggested that ferritinophagy occurred.[47]

Next, we investigated whether the mechanism of esculetin-induced ferritinophagy is associated to regulate of NCOA4, FTH1, LC3-II expression in HUH7 and HCCLM3 cells. We investigated these proteins' role in this process using gene silencing and overexpression. Western blot (Figure 6A and B) and immunofluorescence staining (Figure 6C and D) were used to determine the silencing or over expression efficiencies. After LC3-II targeted silencing, LC3-II expression and green fluorescence in the siLC3-II group considerably decreased compared in the siNC group, there were no noticeable changes in NCOA4 red fluorescence and nearly no yellow spots, suggesting that cellular autophagy was prevented. When esculetin and siLC3-II were combined to treat cells, the colocalization yellow spots and LC3-II green fluorescent significantly increased, suggesting that esculetin adjusted autophagy and triggered ferritinophagy through upregulating LC3-II protein expression. Additionally, the expression of NCOA4 protein and red fluorescence was dramatically decreased (Figure 6A–D), when NCOA4 was silenced. Treatment combination of esculetin and siNCOA4 led to a significant increasing in the expression of NCOA4 red fluorescence and colocalization of yellow spots (Figure 6C and D), compared in the ESC group. These outcomes indicated that esculetin promotes ferritinophagy occurrence by upregulating NCOA4. FTH1 expression in the OEFTH1 group was considerably increased (Figure 6A and B). Furthermore, as compared with the ESC group, the expression of the yellow spots and red fluorescent NCOA4 were substantially decreased in the OEFTH1 and ESC combined group (Figure 6C and D), demonstrating that esculetin causes ferritinophagy by enhancing NCOA4 expression and by promoting FTH1 degradation. The results observed in HUH7

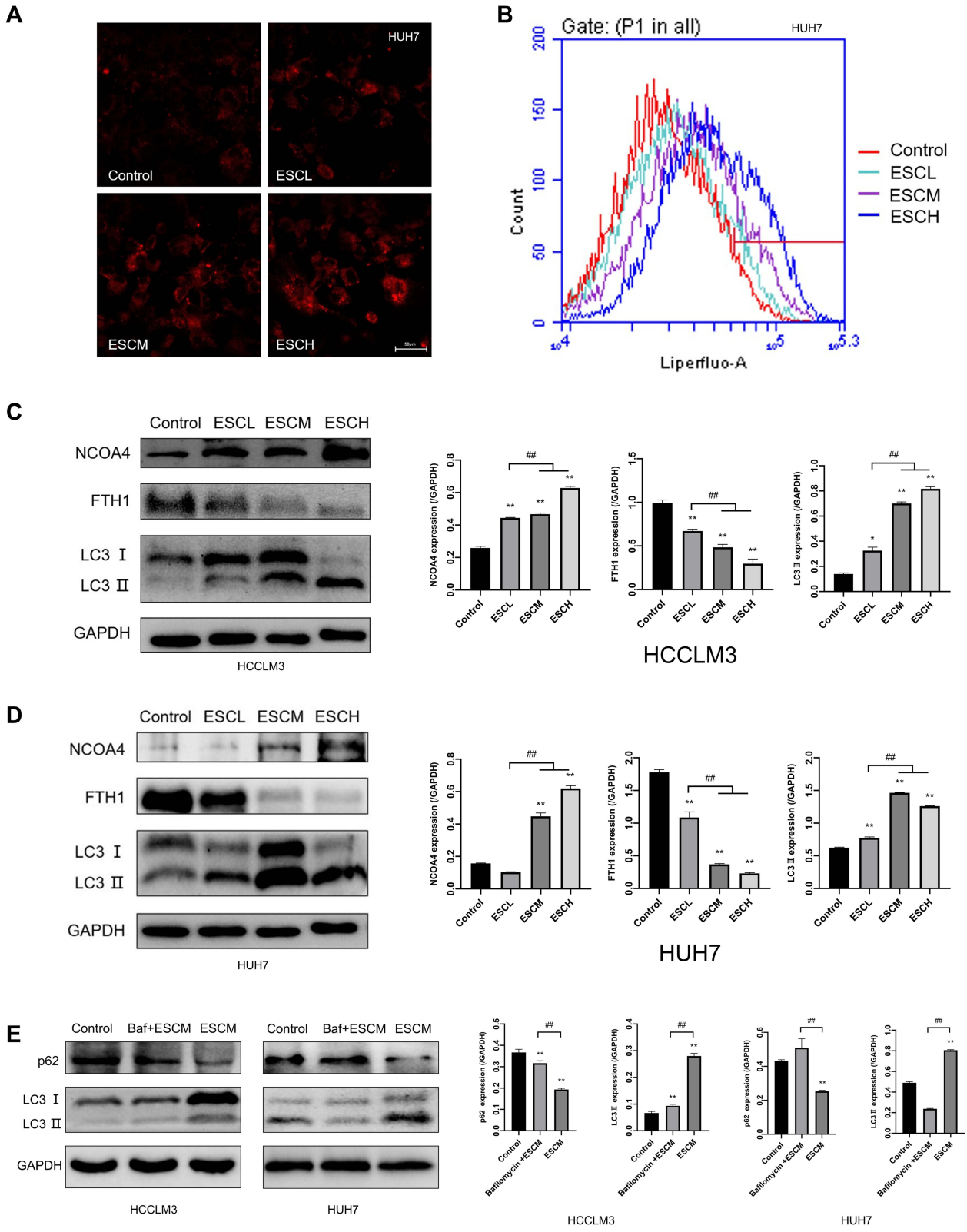

Figure 5 Esculetin's effects on lipid peroxidation and ferritinophagy-proteins in HUH7 and HCCLM3 cells. (**A**) Using the Liperfluo probe and (**B**) flow cytometry, lipid peroxidation was measured in cells. (**C** and **D**) Ferritinophagy-related proteins were detected by Western blot. (**E**) The p62 and LC3-II expressions in cells after Baf and ESCM co-treatment were examined by Western blot. The results were displayed as mean ± SD. Compared with the Control group, *p<0.05, **p<0.01. Compared with the ESCL group, ##p<0.01. Compared with the bafilomycin +ESCM group in E, ##p<0.01.

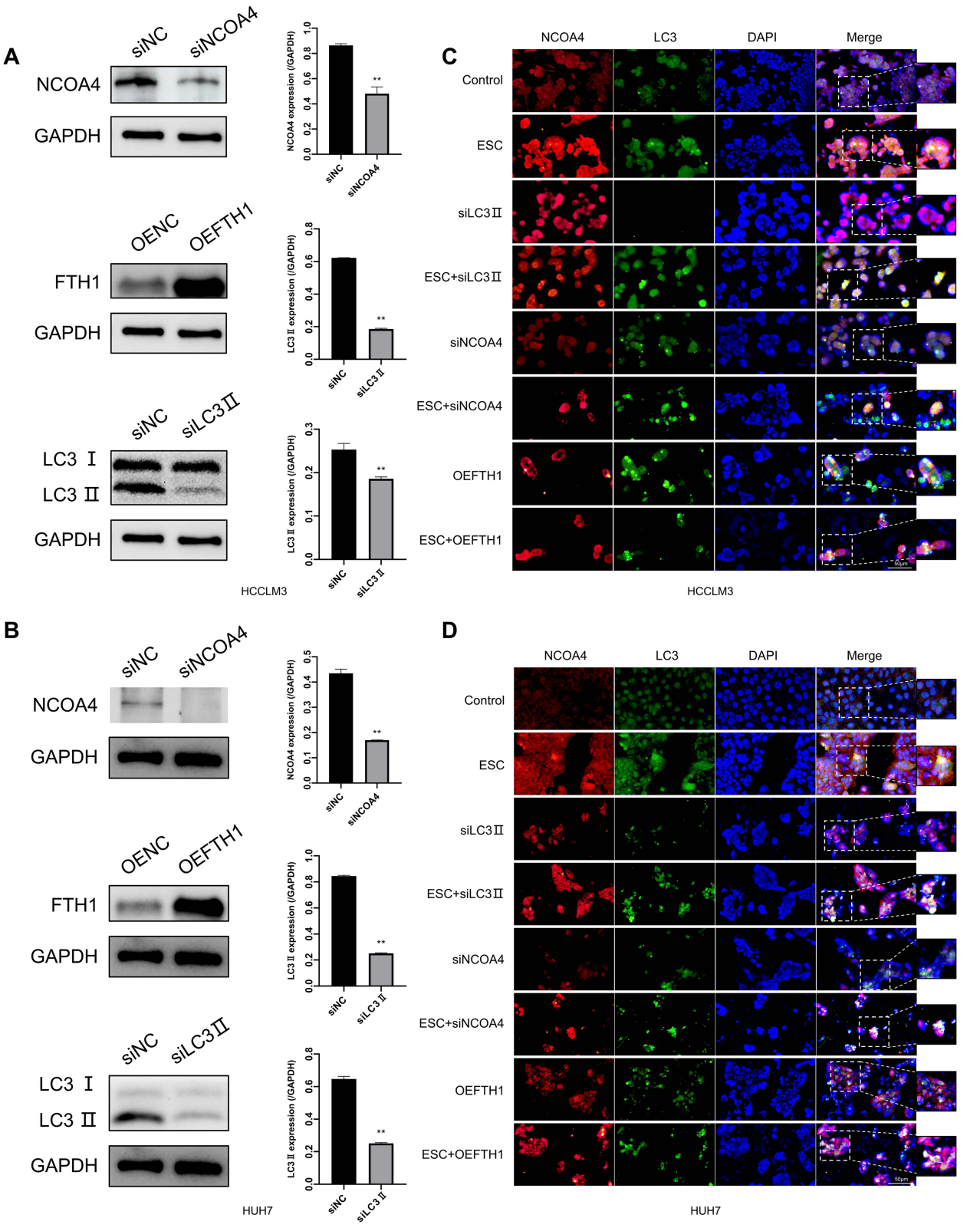

Figure 6 Esculetin's effects on ferritinophagy colocalization following siNCOA4 silencing, OEFTH1 overexpression and siLC3II silencing in HUH7 and HCCLM3 cells. (**A** and **B**) The efficiencies of siNCOA4, siLC3II and OEFTH1 overexpression were detected using Western blot. (**C** and **D**) With immunofluorescence staining, the influences of Esculetin, siNCOA4, siLC3II and OEFTH1 on LC3II and NCOA4 co-localization expression were all analyzed. The results were displayed as mean ± SD. Compared with the siNC or OENC group, ** p<0.01.

cells were similar to those of HCCLM3 cells. Ultimately, esculetin could cause ferritinophagy, promote ferroptosis in HUH7 and HCCLM3 cells, influence NCOA4, FTH1 and LC3-II protein expression levels.

In vivo, Esculetin's Effects on Hepatocellular Cancer and Inducing Ferritinophagy

To establish a hepatocellular cancer animal model that subcutaneous transplantation of HUH7 cell, nude mice were used. Compared in the control group, the findings revealed that the treatment of mice with 3 distinct doses (10 mg/kg, 30 mg/kg and 60 mg/kg) of esculetin had a trend to increase the body weight of the nude mice (Figure 7A). Compared with the control group, the esculetin groups (10 mg/kg, 30 mg/kg and 60 mg/kg) seemly had greater tumour inhibition rates, indicating that esculetin may inhibit growth of hepatocellular cancer in vivo (Figure 7B).

Esculetin 3 groups had a significant reduction in the ability of hydroxyl radical inhibition and GSH (Figure 7C), when compared with the control group. According to the biochemical data analysis of ferroptosis markers in nude mice's serum (Figure 7D), esculetin dramatically improved Fe^{2+} content (Figure 7E) and MDA level in serum (Figure 7F), indicating that esculetin reduces antioxidant capacity in vivo. Using microscope viewed the significantly presence of blue iron deposition by Prussian blue staining in the tumour sections (Figure 7G), demonstrating that esculetin led to lipid peroxidation in vivo and caused iron overload and deposition in tumour tissue.

Using H&E tissue staining, esculetin was tested to see if it produces pathological alterations in mice internal organs, compared in the control group (Figure 7H), there were no significant pathological changes in the heart, liver, lung, spleen, or kidney in the esculetin 3 groups.

Esculetin's impact on the expression levels of proteins associated with oxidation and ferritinophagy in tumour tissue was examined by immunohistochemistry. The results showed that esculetin (30 mg/kg or 60 mg/kg) significantly decreased the number of Ki67 positive cells (Figure 8A and B), compared with the control group, this suggested that esculetin suppresses the proliferation of tumours. When compared with the control group (Figure 8C and D), NFE2L2, GPX4 and HO-1's protein expression levels were substantially lower in the esculetin 3 groups, indicating that esculetin decreases antioxidation level in tumours. Compared with the control group, esculetin (10 mg/kg, 30 mg/kg and 60 mg/kg) significantly increased the protein expression levels of LC3II, NCOA4 and decreased FTH1 expression (Figure 8E and F), suggesting that esculetin has the ability to induce ferritinophagy in cells. In conclusion, esculetin reduces antioxidation level in tumour, promotes ferritin degradation, improves ferritinophagy-related protein levels and activates ferritinophagy to promote ferroptosis in hepatocellular cancer cells.

Discussion

Ferritinophagy results in iron overload in tumour cells, which promotes tumour cell ferroptosis.[48–50] Esculetin is a natural dihydroxy coumarin that is distributed in a variety of plants,[21–25] such as marine sponge. Studies showed that it has inhibitory effects on various tumours and its antitumoral mechanism involves the activation of cellular processes, such as apoptosis.[24–32] However, esculetin's effects of activating ferritinophagy in liver cancer to has never been studied and its mechanism is unidentified.

In our study, we show that esculetin suppresses the growth of HUH7 and HCCLM3 cells, inhibits cell proliferation and migration, increases cell apoptosis levels. With the results of previous research,[51–54] ferroptosis and oxidative stress are intimately related, the feature of ferroptosis is the harmful accumulation of lipid peroxidation. Ferritinophagy increases intracellular Fe^{2+} levels that initiate the Fenton reaction to produce ROS, leading to an increase in oxidative stress and GSH level, resulting in the ferroptosis. In our experiments (Figure 9), esculetin increased ROS production in HUH7 and HCCLM3 cells in a dose-related way, decreased the intracellular-free radical scavenging, reduced antioxidant activity. NFE2L2 has been identified to control ferroptosis through regulating GPX4, FTH1 and HO-1 in cells.[55] In this study, esculetin decreased NFE2L2 expression in vivo and in vitro, which suppressed HO-1, GPX4 and GSH expressions and the scavenge hydroxyl radicals' ability within serum, therefore, influencing the antioxidant levels in tumour tissue. The in vivo and vitro experiments demonstrated that esculetin regulates the level of Fe^{2+}, promotes the production of lipid peroxidation and MDA, increases iron deposition in tumour tissue and causes iron overloading. It has been shown that NCOA4 directly interacts with FTH1, then connects to the LC3 protein on the forming membrane of autophagy and selects the ferritin iron-contained complexes for autolysis, leading to ferroptosis, this is the mechanism by which NCOA4

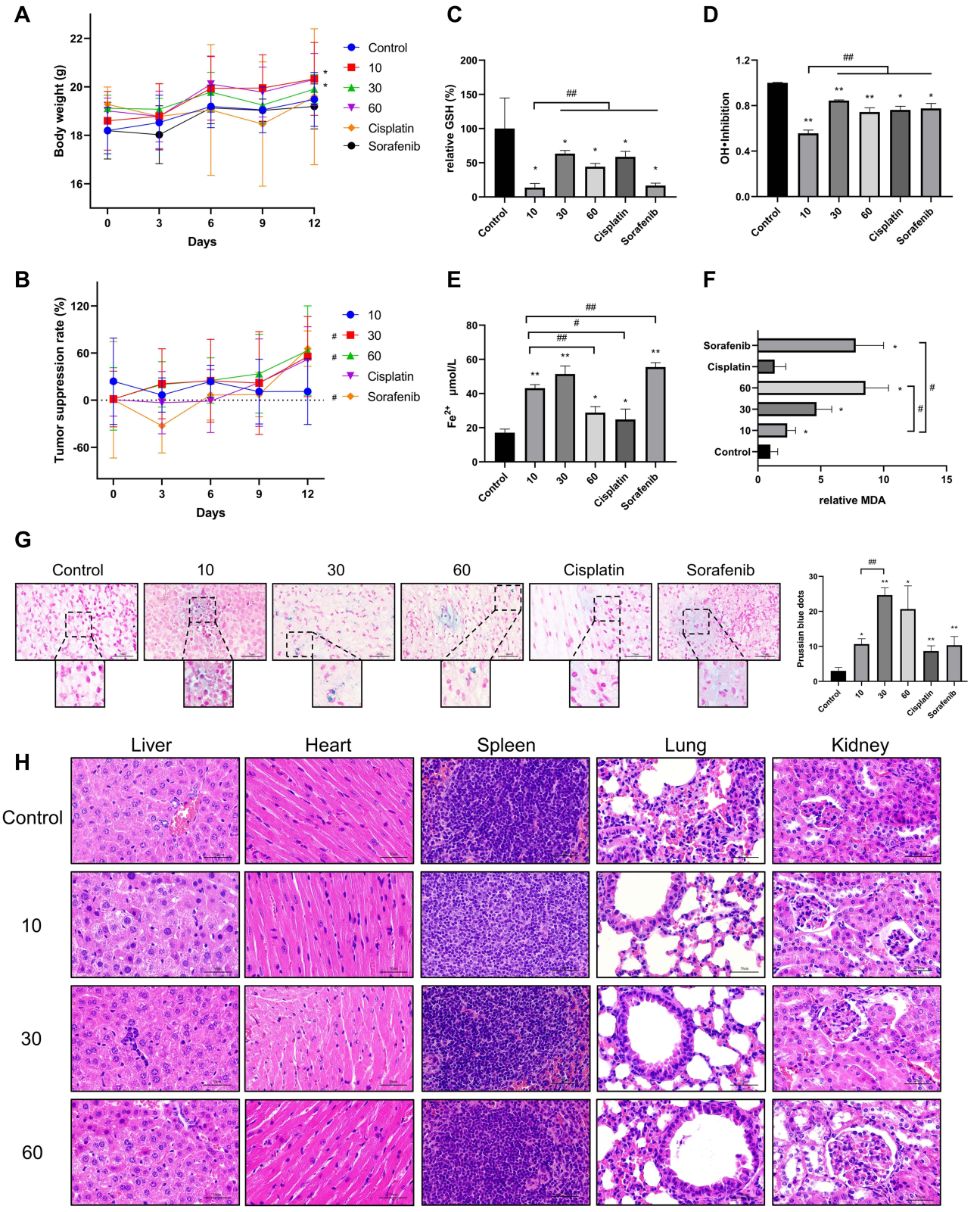

Figure 7 Esculetin's effects on hepatocellular cancer in vivo. (**A**) Every three days, mice's body weight was recorded. (**B**) The implanted tumor's length and width were recorded 5 times and expressed as suppression rate. (**C** and **D**), (**E** and **F**) When the study ended, serum was analyzed for hydroxyl radical inhibition ability, GSH, Fe^{2+} and MDA. (**G**) The iron deposition of ferritinophagy-phenomenon in tumour tissues was confirmed using Prussian blue staining. (**H**) The esculetin-induced pathological changes in the lung, heart, liver, spleen and kidneys of nude mice were observed by H&E staining. The scale bar represents 50 μm (n=3). The results were displayed as mean ± SD. Compared with the Control group, *p<0.05, **p<0.01. Compared with the 10mg/kg group, #p<0.05, ##p<0.01.

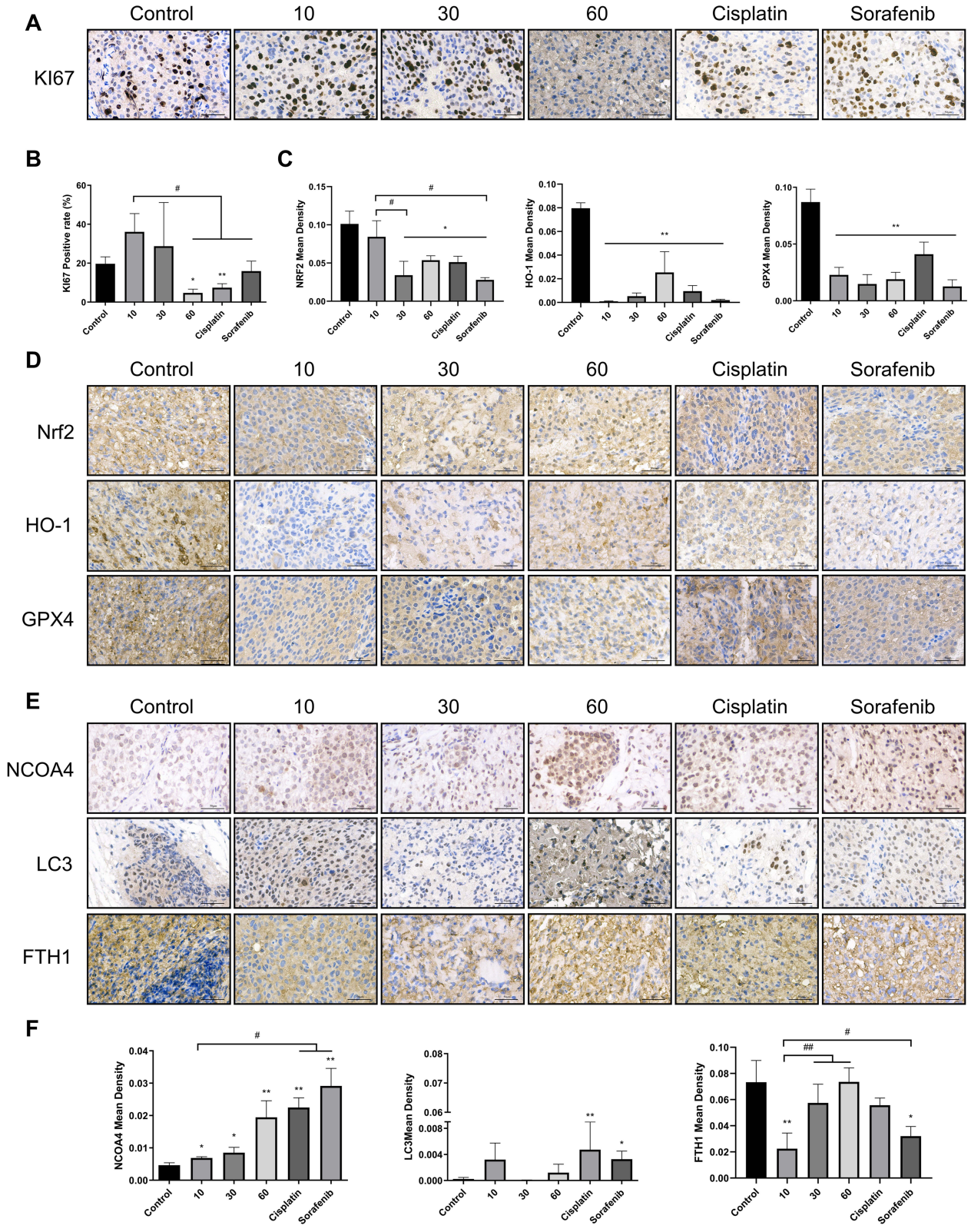

Figure 8 Esculetin's effects on hepatocellular cancer proteins expression in vivo. Using immunohistochemistry, (**A** and **B**) KI67 expression, (**C** and **D**) antioxidant protein NFE2L2, GPX4 and HO-1 expression, (**E** and **F**) ferritinophagy-proteins NCOA4, FTH1 and LC3 expression were measured. The ruler measures 50μm. The results were displayed as mean ± SD (n=3). Compared with the Control group, *p<0.05, **p<0.01. Compared with the 10mg/kg group, $^{\#}$p<0.05, $^{\#\#}$p<0.01.

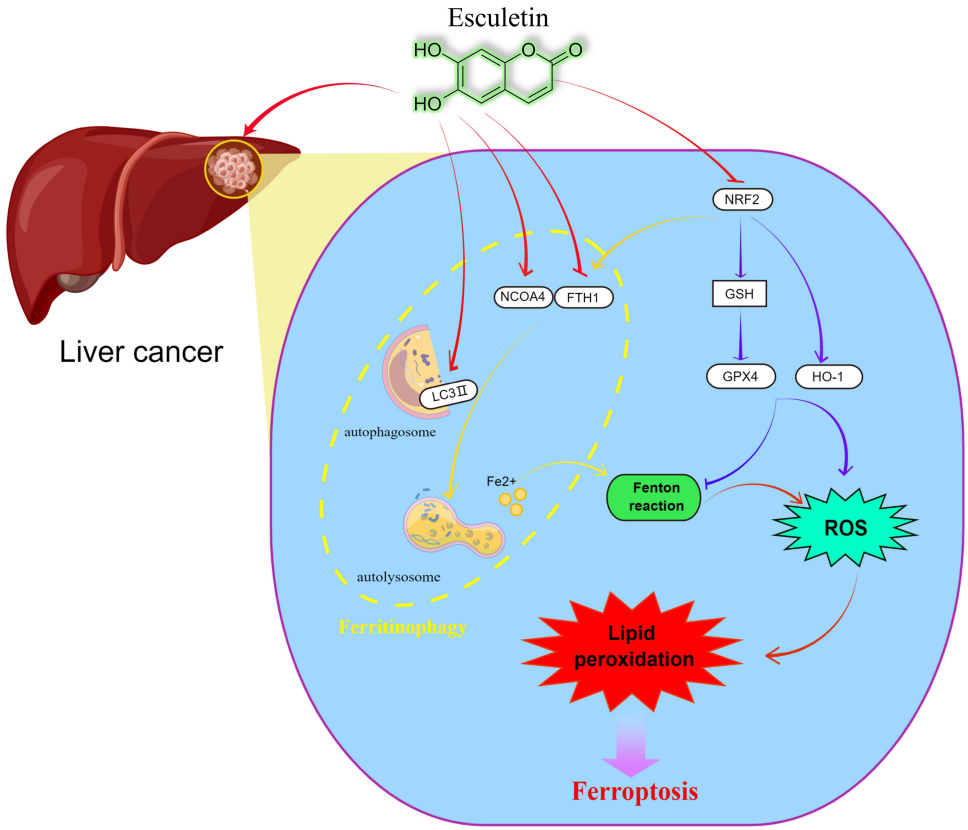

Figure 9 Esculetin can control NCOA4 and FTH1 expressions, regulate lysosomes and LC3-II activities to increase the level of autophagy and induce ferritinophagy to modify ferritin to produce Fe^{2+}. The Fenton reaction leads to the production of the hydroxyl radical, as a consequence of the cell iron accumulating, resulting in oxidative stress and increasing in ROS production. A high production of cell ROS can lead to lipid peroxidation and ferritinophagy. Meanwhile, esculetin can decrease GSH expression by suppressing NFE2L2 and its target protein GPX4 expression, which is the main ferroptosis regulator. Esculetin can also suppress the expressions of the GPX4 target proteins, FTH1 and HO-1, promote ROS buildup and finally activate ferroptosis that is caused by ferritinophagy. By figdraw (www.figdraw.com).

mediates ferritinophagy.[4,56] Inhibiting NCOA4 expression or autophagy can prevent ferritinophagy and ferroptosis.[57] In this study, we observed that esculetin increases the levels of NCOA4, LC3-II and lysosomes, while also decreasing FTH1 expression in vivo and vitro. Esculetin's relationship to ferritinophagy was further verified using gene silencing or overexpression method, we observed that esculetin suppresses the expression of FTH1 following overexpression, while increasing the expressions of NCOA4 and LC3II following silencing. Esculetin was also shown to increase the co-expression of NCOA4 and LC3II, leading to ferritinophagy. Therefore, esculetin can increase free iron level within the cell by activating ferritinophagy. Our research indicates that esculetin can suppress the growth of liver cancer HUH7 and HCCLM3 cells via inducing ferritinophagy that is controlled by the NCOA4 /LC3II /FTH1 signaling pathway in tumour cells, promoting cell ferroptosis.

Despite the meticulous testing, we performed to demonstrate that esculetin activates ferritinophagy to inhibit proliferation of HUH7 and HCCLM3 cells, there are still limits to our research. Esculetin was only proven to induce ferritinophagy in liver cancer cells via the NCOA4/LC3II/FTH1 pathway, but it is uncertain whether esculetin promotes ferritinophagy via other pathways or if it inhibits other cancers. Future experiments should investigate various cancers and pathways to better study esculetin's antitumor effectiveness. In summary, we believe that the small-molecule compound, esculetin, which is present in numerous plants, will be applied as a potential drug to treat liver cancer.

Ethical Statement

Animal experiments in this study were handled in compliance with the Animal Ethics Procedures and Guidelines of the People's Republic of China. All of the animal protocols in this study were approved by the Institutional Animal Care and Use committee (IACUC) of the Changchun University of Chinese Medicine.

Acknowledgments

The authors would like to express their gratitude to EditSprings (https://www.editsprings.cn) for the expert linguistic services provided.

Author Contributions

All authors made a significant contribution to the work reported, whether that is in the conception, study design, execution, acquisition of data, analysis and interpretation, or in all these areas; took part in drafting, revising or critically reviewing the article; gave final approval of the version to be published; have agreed on the journal to which the article has been submitted; and agree to be accountable for all aspects of the work.

Funding

This work was supported by the Natural Science Foundation of Jilin Province (Grant No. YDZJ202201ZYTS257), the Science and Technology Research Planning Project of Jilin Provincial Department of Education (Grant No. JJKH20220887KJ), the Jilin Science and Technology Development Plan Project (NO. 20220508075RC), the Technology Project for Major Disease Prevention and Control in Jilin Province (Grant No. 20210303002SF) and the Jilin Province Traditional Chinese Medicine Science and Technology Project (Grant No. 2022124), the Jilin Province Youth Scientific and Technological Talent Support Project (Grant No. QT202111).

Disclosure

All authors declare that they have no conflict of interests concerning this article.

References

1. Tsurusaki S, Tsuchiya Y, Koumura T, et al. Hepatic ferroptosis plays an important role as the trigger for initiating inflammation in nonalcoholic steatohepatitis. *Cell Death Dis*. 2019;10(6):449. doi:10.1038/s41419-019-1678-y
2. Mancias JD, Wang X, Gygi SP, Harper JW, Kimmelman AC. Quantitative proteomics identifies NCOA4 as the cargo receptor mediating ferritinophagy. *Nature*. 2014;509(7498):105–109. doi:10.1038/nature13148
3. Santana-Codina N, Mancias JD. The role of NCOA4-mediated ferritinophagy in health and disease. *Pharmaceuticals*. 2018;11(4):114. doi:10.3390/ph11040114
4. Mancias JD, Pontano Vaites L, Nissim S, et al. Ferritinophagy via NCOA4 is required for erythropoiesis and is regulated by iron dependent HERC2-mediated proteolysis. *Elife*. 2015;4:e10308.
5. Nai A, Lidonnici MR, Federico G, et al. NCOA4-mediated ferritinophagy in macrophages is crucial to sustain erythropoiesis in mice. *Haematologica*. 2021;106(3):795–805. doi:10.3324/haematol.2019.241232
6. Shen Z, Liu T, Li Y, et al. Fenton-reaction-acceleratable magnetic nanoparticles for ferroptosis therapy of orthotopic brain tumors. *ACS Nano*. 2018;12(11):11355–11365. doi:10.1021/acsnano.8b06201
7. He YJ, Liu XY, Xing L, Wan X, Chang X, Jiang HL. Fenton reaction-independent ferroptosis therapy via glutathione and iron redox couple sequentially triggered lipid peroxide generator. *Biomaterials*. 2020;241:119911. doi:10.1016/j.biomaterials.2020.119911
8. Yoshida M, Minagawa S, Araya J, et al. Involvement of cigarette smoke-induced epithelial cell ferroptosis in COPD pathogenesis. *Nat Commun*. 2019;10(1):3145. doi:10.1038/s41467-019-10991-7
9. Jhelum P, Santos-Nogueira E, Teo W, et al. Ferroptosis mediates cuprizone-induced loss of oligodendrocytes and demyelination. *J Neurosci*. 2020;40(48):9327–9341. doi:10.1523/JNEUROSCI.1749-20.2020
10. Ursini F, Maiorino M. Lipid peroxidation and ferroptosis: the role of GSH and GPx4. *Free Radic Biol Med*. 2020;152:175–185. doi:10.1016/j.freeradbiomed.2020.02.027
11. Chen X, Li J, Kang R, Klionsky DJ, Tang D. Ferroptosis: machinery and regulation. *Autophagy*. 2021;17(9):2054–2081. doi:10.1080/15548627.2020.1810918
12. Siegel RL, Miller KD, Jemal A. Cancer statistics, 2020. *CA Cancer J Clin*. 2020;70(1):7–30. doi:10.3322/caac.21590
13. Anwanwan D, Singh SK, Singh S, Saikam V, Singh R. Challenges in liver cancer and possible treatment approaches. *Biochim Biophys Acta Rev Cancer*. 2020;1873(1):188314. doi:10.1016/j.bbcan.2019.188314
14. Liu CY, Chen KF, Chen PJ. Treatment of liver cancer. *Cold Spring Harb Perspect Med*. 2015;5(9):a021535.
15. Llovet JM, De Baere T, Kulik L, et al. Locoregional therapies in the era of molecular and immune treatments for hepatocellular carcinoma. *Nat Rev Gastroenterol Hepatol*. 2021;18(5):293–313. doi:10.1038/s41575-020-00395-0
16. Zheng Y, Wang S, Cai J, Ke A, Fan J. The progress of immune checkpoint therapy in primary liver cancer. *Biochim Biophys Acta Rev Cancer*. 2021;1876(2):188638. doi:10.1016/j.bbcan.2021.188638
17. Liu Z, Liu X, Liang J, et al. Immunotherapy for hepatocellular carcinoma: current status and future prospects. *Front Immunol*. 2021;12:765101. doi:10.3389/fimmu.2021.765101
18. Terashima T, Yamashita T, Takata N, et al. Comparative analysis of liver functional reserve during lenvatinib and sorafenib for advanced hepatocellular carcinoma. *Hepatol Res*. 2020;50(7):871–884. doi:10.1111/hepr.13505

19. Casadei-Gardini A, Scartozzi M, Tada T, et al. Lenvatinib versus sorafenib in first-line treatment of unresectable hepatocellular carcinoma: an inverse probability of treatment weighting analysis. *Liver Int*. 2021;41(6):1389–1397. doi:10.1111/liv.14817
20. Zhang L, Xie Q, Li X. Esculetin: a review of its pharmacology and pharmacokinetics. *Phytother Res*. 2022;36(1):279–298. doi:10.1002/ptr.7311
21. Hamoda AM, Fayed B, Ashmawy NS, El-Shorbagi AA, Hamdy R, Soliman SSM. Marine sponge is a promising natural source of anti-SARS-CoV-2 scaffold. *Front Pharmacol*. 2021;12:666664. doi:10.3389/fphar.2021.666664
22. Kadakol A, Sharma N, Kulkarni YA, Gaikwad AB. Esculetin: a phytochemical endeavor fortifying effect against non-communicable diseases. *Biomed Pharmacother*. 2016;84:1442–1448. doi:10.1016/j.biopha.2016.10.072
23. Jeong NH, Yang EJ, Jin M, et al. Esculetin from Fraxinus rhynchophylla attenuates atopic skin inflammation by inhibiting the expression of inflammatory cytokines. *Int Immunopharmacol*. 2018;59:209–216. doi:10.1016/j.intimp.2018.04.005
24. Mesas C, Martinez R, Ortiz R, et al. Antitumor effect of the ethanolic extract from seeds of Euphorbia lathyris in colorectal cancer. *Nutrients*. 2021;13(2):566. doi:10.3390/nu13020566
25. Ren W, Zhou Q, Yu R, Liu Z, Hu Y. Esculetin inhibits the pyroptosis of microvascular endothelial cells through NF-kappaB /NLRP3 signaling pathway. *Arch Biochem Biophys*. 2022;720:109173. doi:10.1016/j.abb.2022.109173
26. Rubio V, Garcia-Perez AI, Herraez A, Diez JC. Different roles of Nrf2 and NFKB in the antioxidant imbalance produced by esculetin or quercetin on NB4 leukemia cells. *Chem Biol Interact*. 2018;294:158–166. doi:10.1016/j.cbi.2018.08.015
27. Jiang R, Su G, Chen X, et al. Esculetin inhibits endometrial cancer proliferation and promotes apoptosis via hnRNPA1 to downregulate BCLXL and XIAP. *Cancer Lett*. 2021;521:308–321. doi:10.1016/j.canlet.2021.08.039
28. Zhu X, Gu J, Qian H. Esculetin attenuates the growth of lung cancer by downregulating wnt targeted genes and suppressing NF-kappaB. *Arch Bronconeumol*. 2018;54(3):128–133. doi:10.1016/j.arbres.2017.09.005
29. Arora R, Sawney S, Saini V, Steffi C, Tiwari M, Saluja D. Esculetin induces antiproliferative and apoptotic response in pancreatic cancer cells by directly binding to KEAP1. *Mol Cancer*. 2016;15(1):64. doi:10.1186/s12943-016-0550-2
30. Wang G, Lu M, Yao Y, Wang J, Li J. Esculetin exerts antitumor effect on human gastric cancer cells through IGF-1/PI3K/Akt signaling pathway. *Eur J Pharmacol*. 2017;814:207–215. doi:10.1016/j.ejphar.2017.08.025
31. Li Y, Song W, Ou X, et al. Breast cancer resistance protein and multidrug resistance protein 2 determine the disposition of esculetin-7-O-glucuronide and 4-methylesculetin-7-O-glucuronide. *Drug Metab Dispos*. 2019;47(3):203–214. doi:10.1124/dmd.118.083493
32. Zamojc K, Zdrowowicz M, Hac A, et al. Dihydroxy-substituted coumarins as fluorescent probes for nanomolar-level detection of the 4-amino-TEMPO spin label. *Int J Mol Sci*. 2019;20(15):3802. doi:10.3390/ijms20153802
33. Pan H, Wang BH, Lv W, Jiang Y, He L. Esculetin induces apoptosis in human gastric cancer cells through a cyclophilin D-mediated mitochondrial permeability transition pore associated with ROS. *Chem Biol Interact*. 2015;242:51–60. doi:10.1016/j.cbi.2015.09.015
34. Wu ST, Liu B, Ai ZZ, et al. Esculetin inhibits cancer cell glycolysis by binding tumor PGK2, GPD2, and GPI. *Front Pharmacol*. 2020;11:379. doi:10.3389/fphar.2020.00379
35. Apel K, Hirt H. Reactive oxygen species: metabolism, oxidative stress, and signal transduction. *Annu Rev Plant Biol*. 2004;55:373–399. doi:10.1146/annurev.arplant.55.031903.141701
36. Kattoor AJ, Pothineni NVK, Palagiri D, Mehta JL. Oxidative stress in atherosclerosis. *Curr Atheroscler Rep*. 2017;19(11):42. doi:10.1007/s11883-017-0678-6
37. Nakai K, Tsuruta D. What are reactive oxygen species, free radicals, and oxidative stress in skin diseases? *Int J Mol Sci*. 2021;22(19):10799. doi:10.3390/ijms221910799
38. Park E, Chung SW. ROS-mediated autophagy increases intracellular iron levels and ferroptosis by ferritin and transferrin receptor regulation. *Cell Death Dis*. 2019;10(11):822. doi:10.1038/s41419-019-2064-5
39. Wei S, Qiu T, Yao X, et al. Arsenic induces pancreatic dysfunction and ferroptosis via mitochondrial ROS-autophagy-lysosomal pathway. *J Hazard Mater*. 2020;384:121390. doi:10.1016/j.jhazmat.2019.121390
40. Stockwell BR, Friedmann Angeli JP, Bayir H, et al. Ferroptosis: a regulated cell death nexus linking metabolism, redox biology, and disease. *Cell*. 2017;171(2):273–285. doi:10.1016/j.cell.2017.09.021
41. Stowe DF, Camara AK. Mitochondrial reactive oxygen species production in excitable cells: modulators of mitochondrial and cell function. *Antioxid Redox Signal*. 2009;11(6):1373–1414. doi:10.1089/ars.2008.2331
42. Su Y, Zhao B, Zhou L, et al. Ferroptosis, a novel pharmacological mechanism of anti-cancer drugs. *Cancer Lett*. 2020;483:127–136. doi:10.1016/j.canlet.2020.02.015
43. Yang L, Wang H, Yang X, et al. Auranofin mitigates systemic iron overload and induces ferroptosis via distinct mechanisms. *Signal Transduct Target Ther*. 2020;5(1):138. doi:10.1038/s41392-020-00253-0
44. Protchenko O, Baratz E, Jadhav S, et al. Iron chaperone poly rC binding protein 1 protects mouse liver from lipid peroxidation and steatosis. *Hepatology*. 2021;73(3):1176–1193. doi:10.1002/hep.31328
45. Su LJ, Zhang JH, Gomez H, et al. Reactive oxygen species-induced lipid peroxidation in apoptosis, autophagy, and ferroptosis. *Oxid Med Cell Longev*. 2019;2019:5080843. doi:10.1155/2019/5080843
46. Dodson M, Castro-Portuguez R, Zhang DD. NRF2 plays a critical role in mitigating lipid peroxidation and ferroptosis. *Redox Biol*. 2019;23:101107. doi:10.1016/j.redox.2019.101107
47. Lin PL, Tang HH, Wu SY, Shaw NS, Su CL. Saponin formosanin C-induced ferritinophagy and ferroptosis in human hepatocellular carcinoma cells. *Antioxidants*. 2020;9:8. doi:10.3390/antiox9080682
48. Ajoolabady A, Aslkhodapasandhokmabad H, Libby P, et al. Ferritinophagy and ferroptosis in the management of metabolic diseases. *Trends Endocrinol Metab*. 2021;32(7):444–462. doi:10.1016/j.tem.2021.04.010
49. Liu J, Kuang F, Kroemer G, Klionsky DJ, Kang R, Tang D. Autophagy-dependent ferroptosis: machinery and regulation. *Cell Chem Biol*. 2020;27(4):420–435. doi:10.1016/j.chembiol.2020.02.005
50. Tang M, Chen Z, Wu D, Chen L. Ferritinophagy/ferroptosis: iron-related newcomers in human diseases. *J Cell Physiol*. 2018;233(12):9179–9190. doi:10.1002/jcp.26954
51. Fuhrmann DC, Mondorf A, Beifuss J, Jung M, Brune B. Hypoxia inhibits ferritinophagy, increases mitochondrial ferritin, and protects from ferroptosis. *Redox Biol*. 2020;36:101670. doi:10.1016/j.redox.2020.101670

52. Yang RZ, Xu WN, Zheng HL, et al. Exosomes derived from vascular endothelial cells antagonize glucocorticoid-induced osteoporosis by inhibiting ferritinophagy with resultant limited ferroptosis of osteoblasts. *J Cell Physiol*. 2021;236(9):6691–6705. doi:10.1002/jcp.30331
53. Hou W, Xie Y, Song X, et al. Autophagy promotes ferroptosis by degradation of ferritin. *Autophagy*. 2016;12(8):1425–1428. doi:10.1080/15548627.2016.1187366
54. Feng J, Li C, Xu R, et al. DpdtC-induced EMT inhibition in MGC-803 cells was partly through ferritinophagy-mediated ROS/p53 pathway. *Oxid Med Cell Longev*. 2020;2020:9762390. doi:10.1155/2020/9762390
55. Sun X, Ou Z, Chen R, et al. Activation of the p62-Keap1-NRF2 pathway protects against ferroptosis in hepatocellular carcinoma cells. *Hepatology*. 2016;63(1):173–184. doi:10.1002/hep.28251
56. Kaur J, Debnath J. Autophagy at the crossroads of catabolism and anabolism. *Nat Rev Mol Cell Biol*. 2015;16(8):461–472. doi:10.1038/nrm4024
57. Gao M, Monian P, Pan Q, Zhang W, Xiang J, Jiang X. Ferroptosis is an autophagic cell death process. *Cell Res*. 2016;26(9):1021–1032. doi:10.1038/cr.2016.95